Zeelie, T. A., Root, A., and Krause, A. O. I., Rh/fibre catalyst for ethene hydroformylation: Catalytic activity and characterisation, Applied Catalysis A: General 285 (2005) 96-109.

Available online at www.sciencedirect.com
SCIENCE DIRECT
Applied Catalysis A: General 285 (2005) 96–109
APPLIED CATALYSIS A: GENERAL
www.elsevier.com/locate/apcata

Rh/fibre catalyst for ethene hydroformylation: Catalytic activity and characterisation

T.A. Zeelie [a,*], A. Root [b], A.O.I. Krause [a]

[a] *Helsinki University of Technology, Laboratory of Industrial Chemistry, P.O. Box 6100, FIN-02015 HUT Espoo, Finland*
[b] *Fortum Oil and Gas Oy, P.O. Box 310, FIN-06101 Porvoo, Finland*

Received 3 December 2004; received in revised form 31 January 2005; accepted 10 February 2005
Available online 5 March 2005

Abstract

A fibre-supported Rh-phosphine catalyst, Fibrecat™, was tested in hydroformylation of ethene and characterised by spectroscopic methods (NMR, DRIFT) before reaction, after pretreatments and after reaction. Fibrecat™ was an active and selective catalyst with 95% selectivity for propanal at 100 °C and 0.5 MPa. Higher temperatures were required to obtain similar activity with unmodified Rh/C and Rh/SiO_2 catalysts, and propanal selectivities remained less than 50%. ^{31}P NMR characterisations suggested that two kinds of Rh-P species were formed on Fibrecat™ during the catalyst preparation: a monophosphine species, Rh(acac)(CO)(PS-PPh_2), and a diphosphine species, $Rh(CO)_2$(PS-$PPh_2)_2$. An activation period of 5–10 h at the beginning of the reaction on Fibrecat™ was required for transformation of the monophosphine and diphosphine species in contact with CO/H_2 to the active Rh-carbonyl hydrides. Evidently, Rh supported on phosphine-modified fibre forms catalytically active Rh-phosphine species with superior activity and selectivity to unmodified Rh catalysts and clearly higher activity than Rh-phosphine supported on silica.

Keywords: Ethene hydroformylation; Fibre supports; Phosphines; Rhodium; Heterogeneous hydroformylation; Deactivation; Pretreatments

1. Introduction

The conversion of alkenes, carbon monoxide and hydrogen into aldehydes and alcohols is called hydroformylation. It is one of the largest scale homogeneously catalysed industrial processes using homogeneous phosphine or phophate-modified rhodium or cobalt carbonyls as catalysts [1,2]. Compared with Rh or Co carbonyls, the modification of catalysts with phosphines increases the formation of linear aldehydes, increases the thermal stability and hydrogenation activity, but decreases the reactivity [1]. Since higher reaction temperatures result in decrease in the normal/branched (*n*/*i*) ratio, modern rhodium oxo-plants operate at temperatures around 120 °C to maintain a high *n*/*i* ratio but still a considerable reaction rate.

In liquid-phase applications, leaching of the active metal into the liquid phase [3–5] has prevented the commercial use of heterogenised catalysts. However, many heterogeneous catalysts supported on a variety of oxides, active carbon and zeolites have been studied for gas-phase hydroformylation [6], where no leaching occurs. In the case of unmodified supported catalysts, a good dispersion of metal improves aldehyde yields and reduces hydrogenation [7–10]. Functionalisation of the support with phosphine ligands is another way to improve aldehyde yields, and also the *n*/*i* ratio of the product aldehydes.

Polymers modified with phosphines or phosphites have been studied as supports in the hydroformylation of various substrates, both with rhodium [11–18] and cobalt catalysts [19]. In fact, higher *n*/*i* ratios have been obtained, e.g. in 1-hexene hydroformylation, on polymer-supported phosphine-modified catalysts compared to homogeneous catalysts, possibly because of a higher localised concentration of phosphine atoms around the Rh centre than in free solution

* Corresponding author. Tel.: +358 9 451 2582; fax: +358 9 451 2622.
E-mail address: tarja.zeelie@hut.fi (T.A. Zeelie).

0926-860X/$ – see front matter © 2005 Elsevier B.V. All rights reserved.
doi:10.1016/j.apcata.2005.02.010

[20]. Similar or higher rates and a higher *n*/*i* ratio for aldehydes have also been obtained in ethene or propene hydroformylation with membrane-supported [21] and carbon-nanotube-supported [22] Rh-phosphine catalysts than with homogeneous $HRh(CO)(PPh_3)_3$.

The Finnish company Smoptech Ltd. [23] have developed a method to prepare polymer supports for catalytic use by radiation grafting with high-energy electrons. These materials are commercially available through Johnson Matthey [24]. The pre-irradiation grafting method that they use minimises the formation of homopolymer and the grafted side chains are not cross-linked [25]. Moreover, polymers of different structure can be used in radiation grafting, for example films, fibres, membranes or beads. Other benefits are high capacity of active sites due to a high extent of grafting and good accessibility of the active sites. In the etherification of bulky C_8 alkenes, the mass-transfer over grafted fibre catalysts was better than over the commercial ion-exchange resin Amberlyst 35 [26]. This type of fibrous polymer-supported sulphonic acid catalyst has also been studied for the esterification of propanoic acid [27] and acetic acid [28].

The purpose of this work was to study the catalytic activity of a novel Rh/fibre catalyst (Fibrecat™) in the vapour-phase hydroformylation of ethene. Pre-irradiation grafting had been used to prepare the phosphine-modified polyethene fibre support and the rhodium precursor had been coordinatively anchored to the phosphine groups of the fibre support. The catalytic activity and selectivity of Fibrecat™ were compared with the catalytic activity and selectivity of impregnated carbon- (Rh/C) and silica-supported (Rh/SiO_2) rhodium catalysts. In addition, a silica-supported phosphine-modified reference catalyst prepared from a Rh-phosphine precursor ($Rh\text{-}PPh_3/SiO_2$) was tested. Fibrecat™ was characterised by DRIFT, ^{31}P NMR and ^{13}C NMR before and after the reaction and after different pretreatments in order to identify the Rh-P species that were formed and explain the activation and deactivation of the catalyst.

2. Experimental

2.1. Catalyst preparation

The Rh/fibre catalysts (Fibrecat™) were supplied by Smoptech Ltd. [29]. The polyethene fibre was grafted with styrene and *p*-styryldiphenylphosphine by pre-irradiation grafting method using high energy electrons. A Rh(acac)$(CO)_2$ (acac: acetylacetonate, pentane-2,4-dionato) precursor was coordinatively anchored on the fibre support from dichloromethane or acetone solution under argon. The metal loading varied from 3 to 7.7 wt.% Rh. The rhodium content of Fibrecat™ is used as a prefix in the name of the catalyst, e.g. 3-Fibrecat™. The phosphorus content of the catalysts was between 1.2 and 3.1 wt.% P. The length of the fibre was <0.25 mm and the diameter was 20 μm. See Table 1 for details of the phosphine-containing Rh catalysts.

Grace 432 silica with a particle size of 0.5–1.0 mm, surface area of 320 $m^2\ g^{-1}$ and a pore volume of 1.2 $cm^3\ g^{-1}$ was used as a support for the silica-supported catalysts. For the preparation of 2-$Rh\text{-}PPh_3/SiO_2$ (Smoptech Ltd.), the silica support was dried for 1 h at 250 °C and allowed to cool down to room temperature under vacuum before the incipient wetness impregnation. The Rh(acac)$(CO)PPh_3$ precursor was dissolved in dichloromethane under nitrogen and added to the support during mixing. The catalyst was dried under vacuum to constant weight.

For the preparation of Rh/SiO_2, the silica support was pre-wetted with water–ethanol solution (50:50) and dried overnight at 120 °C and further in vacuum at 0.1–0.4 kPa and 210 °C for 4 h. The catalyst was prepared by incipient wetness impregnation from an aqueous solution of $Rh(NO_3)_3$, and dried at 500 Pa and 60 °C for 2 h. The resulting 6-Rh/SiO_2 catalyst was further dried under 5% O_2/N_2 flow at 120 °C for 6 h, calcined under 5% O_2/N_2 flow at 400 °C for 6 h and reduced under H_2/Ar flow at 300 °C for 3 h before the reaction.

The carbon supported catalysts were prepared [30] and characterised [7,30] previously. The catalysts were prepared by incipient wetness impregnation from an aqueous solution of $Rh(NO_3)_3$. The Rh/C catalysts (Ø = 0.3–0.8 mm) were calcined under nitrogen flow at 400 °C for 3 h and reduced under H_2/Ar flow at 400 °C for 1 h before the reaction. The metal contents of the catalysts were 7.7 wt.% Rh for Rh/C(C) (coconut-based carbon from Johnson Matthey) and 6.7 wt.% Rh for Rh/C(T) (wood-based carbon from Takeda Shirasaki).

2.2. Catalyst characterisation

2.2.1. Chemisorption

The hydrogen uptake of the reduced 6-Rh/SiO_2 was measured at 30 °C with static volumetric chemisorption equipment, Coulter OMNISORP 100CX, by the method reported elsewhere in detail [30] and here only briefly. Before the measurement, the catalyst was reduced in situ in flowing hydrogen at 300 °C for 3 h. The amount of strongly adsorbed hydrogen representing irreversible chemisorption was determined by subtracting the isotherm of reversible adsorption from the isotherm of total adsorption. The dispersion was calculated from the irreversible uptake of hydrogen after correction for the extent of reduction measured by oxygen titration. The oxygen titration of the reduced catalyst was carried out by performing static volumetric chemisorption measurements at 400 °C using a 20 vol.% O_2/He gas mixture. Metallic rhodium was assumed to fully oxidise to Rh_2O_3 under these conditions. The dispersions for Rh/SiO_2 and Rh/C(C) from hydrogen chemisorption were 59 and 27% [9], respectively, and the extents of reduction were 85 and 78% [9].

2.2.2. DRIFT

The catalysts were characterised by diffuse reflectance infrared fourier transform (DRIFT) spectroscopy using a

Table 1
Characteristics of the phosphine-containing Rh catalysts

Catalyst	Rh content (wt.%)	P content (wt.%)[d]	S/P[e]	Rh precursor	Solvent	Mono/di ratio[f]
3-Fibrecat™	2.9[a] (4.0[b])	1.2	10	$Rh(acac)(CO)_2$	Dichloromethane	1.5
4-Fibrecat™	4.4[a] (6.7[b])	1.3	10	$Rh(acac)(CO)_2$	Dichloromethane	1.8
8-Fibrecat™	n.d. (7.7[b])	2.3	10	$Rh(acac)(CO)_2$	Dichloromethane	n.d.
3-Fibrecat™ (Acet)	n.d. (2.8[c])	1.2	10	$Rh(acac)(CO)_2$	Acetone	3.6
4-Fibrecat™ (Acet)	n.d. (4.2[b])	1.2	10	$Rh(acac)(CO)_2$	Acetone	3.2
6-Fibrecat™ (Acet)	n.d. (5.9[c])	3.1	4	$Rh(acac)(CO)_2$	Acetone	5.6
2-Rh-PPh_3/SiO_2	n.d. (2.0[d])	0.6	–	$Rh(acac)(CO)(PPh_3)$	Dichloromethane	–

n.d.: not determined.
[a] Method A (the most accurate method): the catalyst is burned at 900 °C and dissolved in $HCl + Cl_2$ (gas); Rh content is determined by ICP.
[b] Method B: the catalyst is mixed with sodium peroxide and sodiumcarbonate in a Zr crucible and heated on a bunsen burner until the exotermic reaction ceases. The residue is dissolved in H_2O; Rh content is determined by AAS.
[c] Method C: value based on the Rh content of solution after Rh deposition; determined by AAS.
[d] Value given by manufacturer.
[e] Styrene/styryldiphenylphosphine molar ratio.
[f] Molar ratio of the Rh-monophosphine species to the Rh-diphosphine species.

Nicolet Nexos spectrometer and deuteride triglyceride sulfide (DTGS) detector. Spectra were recorded in the wavenumber range of 4000–400 cm^{-1} with a spectral resolution of 2 cm^{-1}. A background spectrum without any sample was always subtracted. The reflectance spectra were measured from catalyst powder at room temperature in air from which carbon dioxide and moisture had been removed. In some cases the catalyst sample was diluted with KBr.

2.2.3. NMR

All the NMR experiments were carried out with a Chemagnetics CMX270 infinity spectrometer. A 6 mm multinuclear probe with zirconia rotors was used for both the ^{13}C and ^{31}P experiments. The ^{31}P CPMAS NMR experiments were carried out using 50 kHz rf fields (5 μs 90° pulse), 5 s recycle delay, 2 ms contact time and spinning speeds between 5 and 7 kHz. The number of transients obtained ranged from 4 to 1000, depending on the sample studied. The same rf field strength were used for the ^{13}C CPMAS NMR spectra and they were acquired using 2 s recycle delay and either a 5 or 2 ms contact time. Between 3000 and 5000 transients were acquired for each spectrum.

Quantitative ^{31}P MAS NMR spectra were also measured. In principle these require that the T_1 relaxation times of all the ^{31}P species in the sample be known so that a sufficient recycle delay can be used to ensure complete relaxation between subsequent acquisitions. In this work the ^{31}P T_1 of the reference sample, styryldiphenylphosphine, the fresh catalyst (4-Fibrecat™) and one of the samples under study, 3-Fibrecat™ after CO/H_2 treatment, were measured to obtain the scale of the T_1 times. Measurements were made using cross-polarisation to the ^{31}P nuclei, followed by an inversion (90°) pulse and a variable relaxation delay to give an inversion recovery type of plot of the magnetisation. The maximum T_1 value for the fibre samples was 50 s, while for the styryldiphenylphosphine it was in excess of 340 s, presumably due to the high degree of crystallinity of this sample.

In addition, spectra of styryldiphenylphosphine were acquired using a direct ^{31}P 36° excitation pulse under the same conditions but with 1000, 2000 and 4000 s recycle delays. No significant increase in signal intensity was found with increased delay. Therefore, for the reference sample, a 1000 s recycle delay was used to acquire the spectra using a direct 36° excitation pulse.

For the Fibrecat™ catalyst samples, a pulse angle of 36° and recycle delay of 60 s were considered adequate for the acquisition of quantitative spectra. With use of these parameters, known amounts of samples were measured and compared with the spectrum of a known amount of the reference material, styryldiphenylphosphine. In this way, the amount of phosphorus present in each sample could be obtained, and deconvolution of the spectra allowed the absolute amounts of each phosphorus species in each sample to be calculated.

2.3. Ethene hydroformylation

The ethene hydroformylation was carried out in an automated fixed bed tubular reactor. In the standard reaction experiments, the Fibrecat™ samples were tested as received without pretreatment. The standard reaction conditions were 0.5 MPa and 100 or 110 °C and the reactor was heated to the reaction temperature under Ar flow. The feed flow was 3.5 or 7 l/h and consisted of 1:2:2:2 molar ratio of Ar (AGA, 99.999%), CO (AGA, 99.97%), H2 (AGA, 99.999%) and C_2H_4 (AGA, 99.95%). In some cases, Ar (7 l/h), CO (Ar:CO = 4:2 l/h), H_2 (Ar:H_2 = 4:2 l/h) or H_2/CO (Ar:CO:H_2 = 4:2:2 l/h) pretreatments were carried out at the reaction temperature. The catalyst amount was 0.5 g, WHSV of ethene 2.5 or 5 1/h and the reaction time was typically 24 h.

The product analysis was carried out on-line with two HP 5890 gas chromatographs; one was equipped with a DB-1 column (30 m × 0.320 mm, film thickness: 3 μm) from J&W Scientific and a PoraplotQ column (25 m × 0.320 mm) from Hewlett-Packard, and the other with a packed column filled with activated carbon coated with 2% squalane. The response factors published by Dietz [31] were used in the quantitative

determinations. The calculation of ethene conversion (X) is based on the molar amount of ethene consumed and the product selectivities (S) were also calculated on molar basis. The condensation products of propanal are denoted by C_6–O, and the oxo-selectivity is defined as the sum of selectivities for propanal, C_6–O and 3-pentanone.

3. Results

3.1. Catalytic activity

3.1.1. Catalyst comparison

The performances of the phosphine-containing Fibrecat™ and 2-Rh-PPh_3/SiO_2 and the non-phosphine modified Rh/C and Rh/SiO_2 catalysts were compared in hydroformylation of ethene at 0.5 MPa and 110 °C. The main products were ethane and propanal. Small amounts of propanol, 3-pentanone and the condensation products of propanal, 2-methyl-2-pentenal and 2-methyl-1-pentanal (C_6–O), were also formed.

Table 2 presents the ethene conversion and product selectivities for the Rh catalysts. The activities of the unmodified Rh catalysts were very low; ethene conversions were 1% or below. Modification of the Rh/SiO_2 catalyst with phosphine improved the activity slightly, and the oxo-selectivity was improved considerably, to 95%. When Rh was supported on phosphine-modified fibre, very high ethene conversion was obtained (46%) and the oxo-selectivity was excellent (S_{oxo} = 93%).

Since the activity of the unmodified Rh catalysts was so low at 110 °C, all the catalysts were also tested at 175 °C. Higher ethene conversions were then obtained with Rh/C(C) [9] and Rh/SiO_2, but the oxo-selectivities deteriorated to 55 and 37%, respectively. Unfortunately, the phosphine-modified silica catalyst deactivated completely at 175 °C, and the temperature was also too high for the fibre-supported catalyst owing to the poor temperature endurance of the fibre support.

The time-on-stream behaviour was clearly different for the non-phosphine-modified catalysts and for Fibrecat™ and 2-Rh-PPh_3/SiO_2. The carbon- and SiO_2-supported rhodium catalysts showed a decreasing activity during the first 5 h of the reaction, after which steady-state conversion was reached (175 °C), whereas the activity of 2-Rh-PPh_3/SiO_2 and Fibrecat™ increased with time on stream (110 °C). Since the performance of Fibrecat™ was so superior compared to the other catalysts, it deserved a more detailed study.

3.1.2. Effect of process conditions

The conversions for 8-Fibrecat™ at three different reaction temperatures are presented in Fig. 1. The temperature of 135 °C was clearly too high: the catalyst deactivated from the initial 60 conversion to 10% conversion in 15 h on stream. There was an initial activation period at every temperature tested and at 110 °C it lasted 15 h (feed 3.5 l/h). The conversion of 9% at 75 °C is comparable to the result of Feldman et al. [21] with a membrane-supported Rh-phosphine catalyst at 80 °C and 0.1 MPa.

The propanal selectivity was excellent for 8-Fibrecat™ at all temperatures tested (see Table 2). The oxo-selectivities were 93–98% and the hydrogenation selectivities to ethane were only 2.5–6.5%. Similarly, in the studies of Feldman et al. [21], the hydrogenation selectivity to ethane was only 1–3% at 80 °C and 0.1 MPa. Even though 8-Fibrecat™ was strongly deactivated at 135 °C, the excellent selectivity to propanal remained unchanged.

The effect of pressure on the activation was investigated in a few experiments carried out at 110 °C and 1.0 MPa (see Fig. 1b). The 8-Fibrecat™ was quickly activated, reaching conversion of 84% after only 3 h on stream, but the fast

Table 2
Ethene conversion and product selectivities in ethene hydroformylation at 0.5 MPa after 20 h

Catalyst	Reaction temperature (°C)/feed (l/h)	Ethene conversion (%)	Product selectivities (%)			
			Ethane	Propanal	C_6O	3-Pentanone
7-Rh/C(C)	110/3.5	1.2	24	58	3.5	15
	175/7	24	45	50	5.0	–
6-Rh/SiO_2	110/3.5	0.7	35	61	3.7	–
	175/7	11	63	35	2.2	–
2-Rh-PPh_3/SiO_2	110/3.5	2.2	5.3	90	0.6	3.7
	175/7	–				
8-Fibrecat™	75/3.5	7.0[a]	2.4	96	1.6	0.2
	110/3.5	46	6.5	88	5.2	0.2
	135/3.5	12	4.8	93	2.3	0.3
3-Fibrecat™	100/7	20	4.1	96	–	–
	110/7	18	3.2	96	0.7	0.1
3-Fibrecat™ (Acet)	100/7	15	4.5	95	0.1	0.1
4-Fibrecat™ (Acet)	100/7	14	4.5	95	0.1	0.1
6-Fibrecat™ (Acet)	100/7	20	6.7	93	0.2	0.1

[a] Reaction time 8 h.

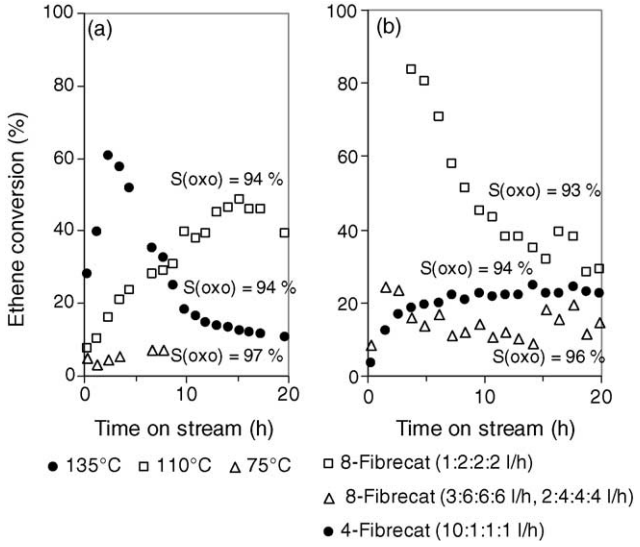

Fig. 1. Ethene conversion with time on stream: (a) for 8-Fibrecat™ at 75–135 °C and 0.5 MPa (feed 3.5 l/h) and (b) for 7- and 8-Fibrecat™ at 110 °C and 1.0 MPa with different feed flows.

activation was followed by deactivation. About 40 wt.% of C_6O and unidentified products longer than C_6 were formed at the beginning of the reaction and may have caused deactivation by blocking the surface. The feed flow was therefore increased as a means of decreasing the conversion level and thus the amount of long-chain products formed. With a feed of 21 l/h ($Ar:CO:H_2:C_2H_4 = 3:6:6:6$ l/h) some deactivation still occurred, even though no long-chain products ($>C_6$) were formed. As a test of the effect of partial pressure of carbon monoxide and hydrogen on the deactivation, the amount of inert Ar in the feed was increased ($Ar:CO:H_2:C_2H_4 = 9.9:1:1:1$ l/h) so that the partial pressure of carbon monoxide and hydrogen was decreased from 0.29 to 0.08 MPa. The reaction was continued at 0.5 MPa and 110 °C and indeed, there was no decrease in conversion. Also, no long-chain products were detected. Thus, the deactivation could be avoided by decreasing the partial pressure of CO and hydrogen in the feed. These results indicate that the partial pressure of carbon monoxide or hydrogen has an effect on the deactivation of the catalyst.

Hydroformylation runs lasting 50 h were carried out to assess the long-term stability of Fibrecat™. As illustrated in Fig. 2, the conversion for 3-Fibrecat™ decreased from 15 to 10% during 50 h at 100 °C and 0.5 MPa. The propanal selectivity increased only slightly, from 94 to 96%. At 110 °C and 0.5 MPa, the deactivation was even more drastic: conversion decreased from 28 to 10% during 40 h on stream.

3.1.3. Effect of pretreatments on the activation of Fibrecat™

The activation of Fibrecat™ at the beginning of the reaction suggests a change in the amount or nature of the active sites with time. The effect of the reacting gases on the activation period was investigated by pretreatments with

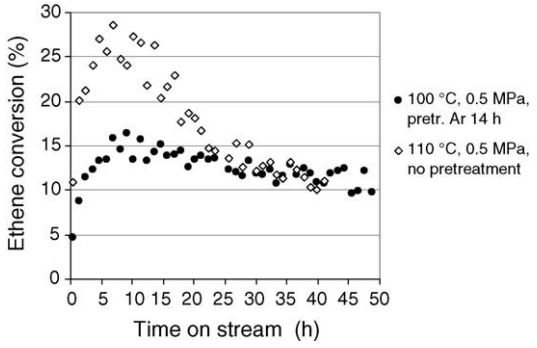

Fig. 2. Ethene conversion for 3-Fibrecat™ at 100 °C and 110 °C and 0.5 MPa (feed 7 l/h).

carbon monoxide, hydrogen and a combination of these at 100 °C and 0.5 MPa. The effect of temperature was studied by pretreatment with argon. As illustrated in Fig. 3, the argon, carbon monoxide and hydrogen pretreatments did not shorten the activation period. After CO/H_2 pretreatment, however, the conversion was already 13% after 20 min and the steady-state conversion was at a lower level (about 18%) than with the other treatments (20%). Similar trend was observed at 110 °C by carbon monoxide pretreatment alone (not shown): relative to the untreated catalyst, the carbon monoxide pretreatment shortened the activation period from 15 to 5 h and the conversion level decreased from 45 to 33% (8-Fibrecat™).

In all, at 110 °C the pretreatment with carbon monoxide and at 100 °C the pretreatment with CO/H_2 shortened the activation period. The accompanying effect, unfortunately, was decreased conversion level. It must be noted that the propanal selectivity remained at 95–96% during the activation period, which means that only the amount of the active sites was changing.

3.1.4. Effect of solvent used during the preparation

Fig. 4 shows the ethene conversion for Fibrecat™ samples prepared by using acetone or dichloromethane as a solvent in the deposition stage of the rhodium precursor. Since the activity and selectivities of 3-Fibrecat™ (Acet) and 4-Fibrecat™ (Acet) were similar, only 3-Fibrecat™

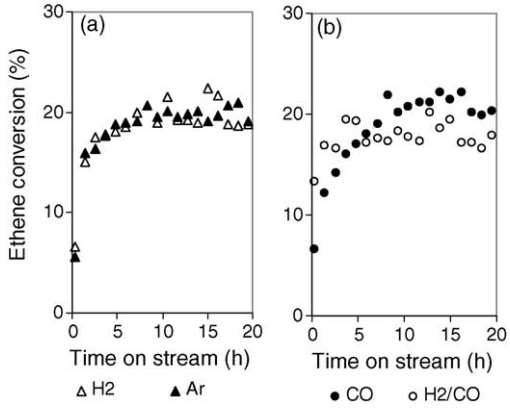

Fig. 3. Ethene conversion for 3-Fibrecat™ at 100 °C and 0.5 MPa (feed 7 l/h) after pretreatment with (a) Ar or H_2 for 7 h and (b) CO or CO/H_2 for 7 h.

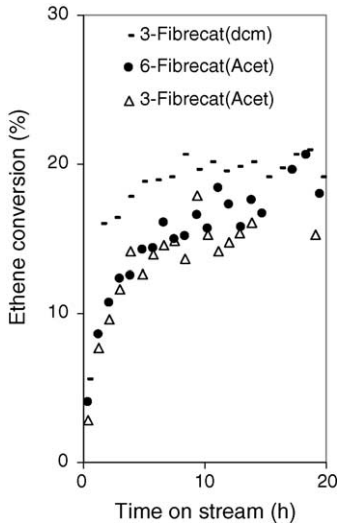

Fig. 4. Ethene conversion at 100 °C and 0.5 MPa for Fibrecat™ samples prepared using acetone (no pretreatment) or dichloromethane (Ar pretreatment for 7 h) for deposition of the Rh precursor.

(Acet) is discussed in the following. The activation behaviour with the samples prepared with acetone was similar to that of the catalysts prepared with dichloromethane, except that the activation took longer for 6-Fibrecat™ (Acet) than for 3-Fibrecat™ (dcm) with similar conversion level. Moreover, the conversion level for 3-Fibrecat™ (Acet) was lower than for 3-Fibrecat™ (dcm). The samples prepared with acetone exhibited different propanal selectivities depending on the metal loading: the propanal selectivity was 95% for 3-Fibrecat™ (Acet), but from 91% (10 h) to 93% (20 h) for 6-Fibrecat™ (Acet).

3.2. Characterisation of Fibrecat™

Since the performance of Fibrecat™ was so much superior to the carbon- and silica-supported Rh catalysts, in terms of both activity and selectivity, the catalyst was characterised in more detail. The structure of the active catalytic species and the changes occurring in the active species during the activation and deactivation were of interest.

3.2.1. Fresh catalyst

The ^{31}P CPMAS NMR spectra of the styryldiphenylphosphine precursor (SDP), the polyethene fibre grafted with styrene and styryldiphenylphosphine, and the resulting catalyst after Rh precursor addition from dichloromethane solution are presented in Fig. 5a–c. The narrow line for *p*-styryldiphenylphosphine at −7.2 ppm (Fig. 5a) moves to −5.3 ppm in the spectrum of the grafted fibre (Fig. 5b) and a new peak appears at 25.3 ppm. The peak at 25.3 ppm is most probably triphenylphosphine oxide [31]. The peaks get broader due to the more amorphous nature of the matrix.

Two types of Rh-P species were formed during the catalyst preparation, as illustrated in Fig. 5c by signals at

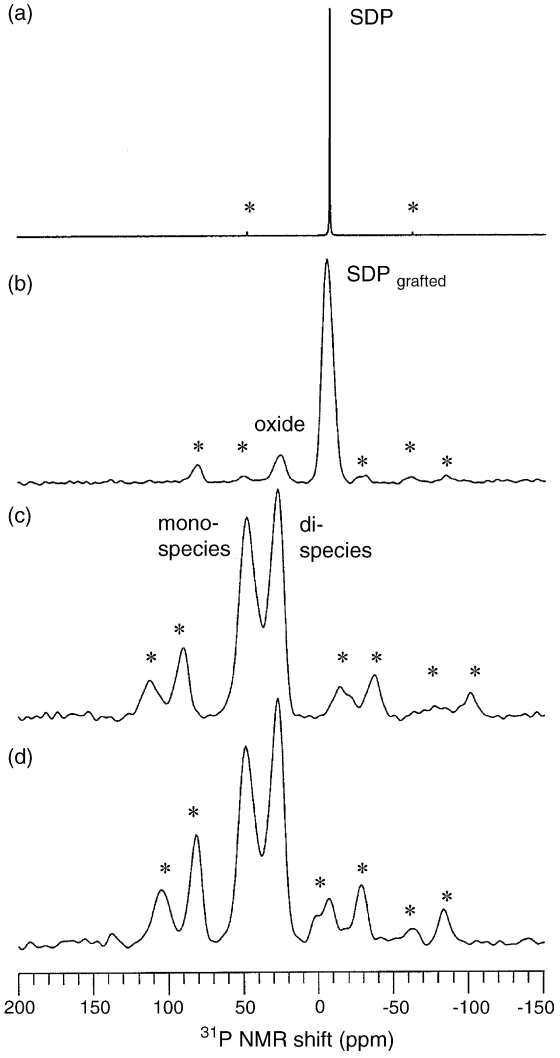

Fig. 5. ^{31}P CPMAS NMR spectra of: (a) styryldiphenylphosphine (SDP); (b) polyethene grafted with styrene and styryldiphenylphosphine; (c) 4-Fibrecat™; and (d) ^{31}P MAS NMR spectrum of 4-Fibrecat™. The spinning sidebands are denoted with asterisks (*).

27.9 and 48.7 ppm. The reaction of $Rh(CO)_2(acac)$ with triphenylphosphines in a 1:1 ratio to form a monophosphine species $Rh(CO)(acac)(PPh_3)$ by CO exchange is well documented in the literature [32]. Accordingly, the peak at 48.7 ppm can be assigned to the monophosphine species, $Rh(CO)(acac)(PS\text{-}PPh_2)$ [33]. See also Scheme 1.

The acac in the monophosphine species can react further with another phosphine group of the support to form a diphosphine species, $Rh(CO)(PS\text{-}PPh_2)_2X$ (Scheme 1). Rh-diphosphine complexes of type *trans*-$Rh(CO)(PPh_3)_2X$ (X is an anion or solvate molecule) typically have resonance lines around 28 ppm [33,34]. In the studies of Malmström et al. [34] with a similar type of catalyst in H_2O/CH_2Cl_2 solution, the second acac phosphine exchange reaction occurred in excess of phosphine since Rh was located in the organic phase and the Rh-phosphine species in the water phase. The existing COO^- groups or $CH_3SO_3^-$ groups in the water phase promoted the reaction and only the diphosphine

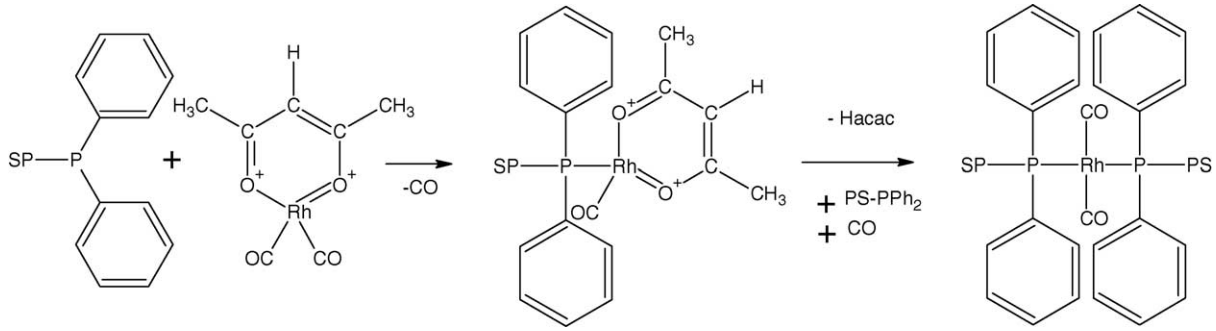

Scheme 1. Schematic presentation of Fibrecat™ preparation.

species was formed. In our case, only dichloromethane is present and there are no anionic groups on the support, but carbon monoxide is released in the first exchange reaction (Scheme 1). Accordingly, the peak at 27.9 ppm is suggested to be a dicarbonyl diphosphine species, $Rh(CO)_2(PS\text{-}PPh_2)_2$.

It could be argued that this peak at 27.9 ppm is just due to a significant amount of trapped styryldiphenylphosphine oxide. However, three pieces of evidence suggest that this is not so, or if present, only in small amounts. Firstly, no change in the ^{31}P MAS NMR spectra is observed over time when exposed to atmosphere. Secondly, ^{31}P relaxation times of the peaks at 25–27 and 47–48 ppm were measured for 3-Fibrecat™ and 4-Fibrecat™. Both species had almost the same relaxation time of around 40–45 s. It might be expected that the free oxide would have quite a different relaxation time due to its unrestricted nature. Indeed, the peak at 27–28 ppm does show evidence for a small amount of shorter ^{31}P T_1 component of about 5 s, which could be due to some residual oxide (see Fig. 6). However, the main component of the 27 ppm peak is the longer relaxing species. Thirdly, the results of the quantitative analysis by ^{31}P NMR and elemental analysis are in better agreement with the assumption that the peak at 27 ppm is due to the diphosphine species. The phosphorus content of the Fibrecat™ can be calculated from the quantified ^{31}P MAS NMR measurements. The P content of 3-Fibrecat™ by NMR was 1.1 wt.%, which was in accordance with the elemental P-analysis of the catalysts (1.2 wt.%). From the wt.% of phosphorus we can calculate the wt.% of rhodium. If the species at 27 ppm is assumed to be a diphosphine species (2P for every Rh), the total amount of phosphorus coordinated Rh would be 2.7 wt.%. If it is a mono species (1P for every Rh) then the total Rh content would be 3.7 wt.%. If a phosphine oxide species is assumed, no Rh is coordinated to it and this would give a total Rh content of 1.6 wt.%. The Rh content of the catalyst determined by elemental analysis was 2.9 wt.% Rh.

The P content for the 4-Fibrecat™ obtained from the quantified ^{31}P MAS NMR measurements was 1.6 wt.% P (elemental analysis: 1.3 wt.% P), which gives 3.9, 5.2 or 2.5 wt.% for the amount of coordinated rhodium, depending whether the 27 ppm peak is due to di, mono, or oxide species. The elemental analysis gives a value of 4.4 wt.% Rh. Thus, the values obtained from ^{31}P MAS NMR results and elemental analysis for the Rh content are in reasonable agreement using the assumption that the peak at 27 ppm is mainly due to the diphosphine species.

Some Fibrecat™ samples were prepared using acetone as solvent. Clearly, the Rh-phosphine distribution has changed relative to Fibrecat™ prepared from dichloromethane (see Fig. 7). Although the CPMAS method was used here, the peak ratios are almost the same as those obtained with the MAS method (see, e.g. Fig. 5c and d). We assume, therefore, that the peak ratios obtained from the CPMAS NMR spectra are a good approximation of the ratios measured using MAS

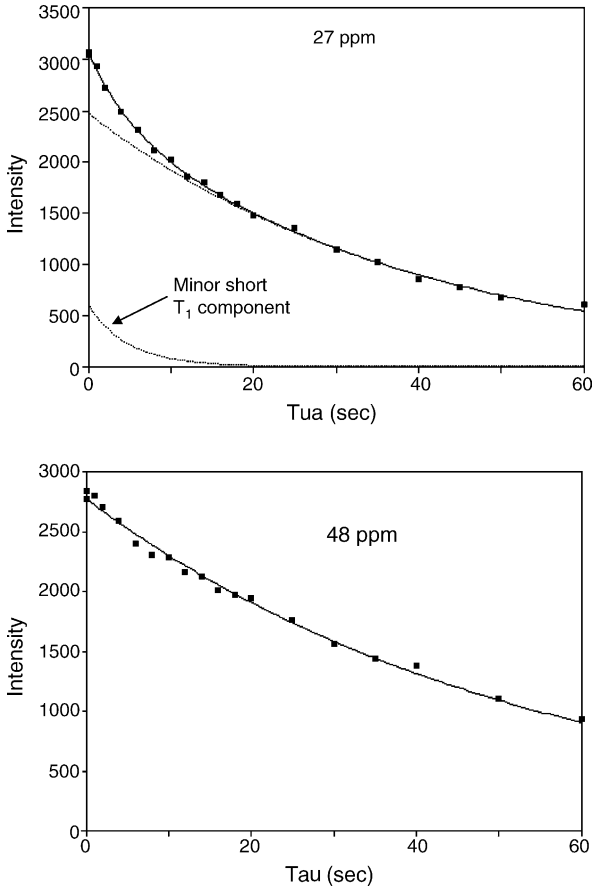

Fig. 6. ^{31}P T_1 relaxation fits for the peaks at 27 and 48 ppm in 4-Fibrecat™.

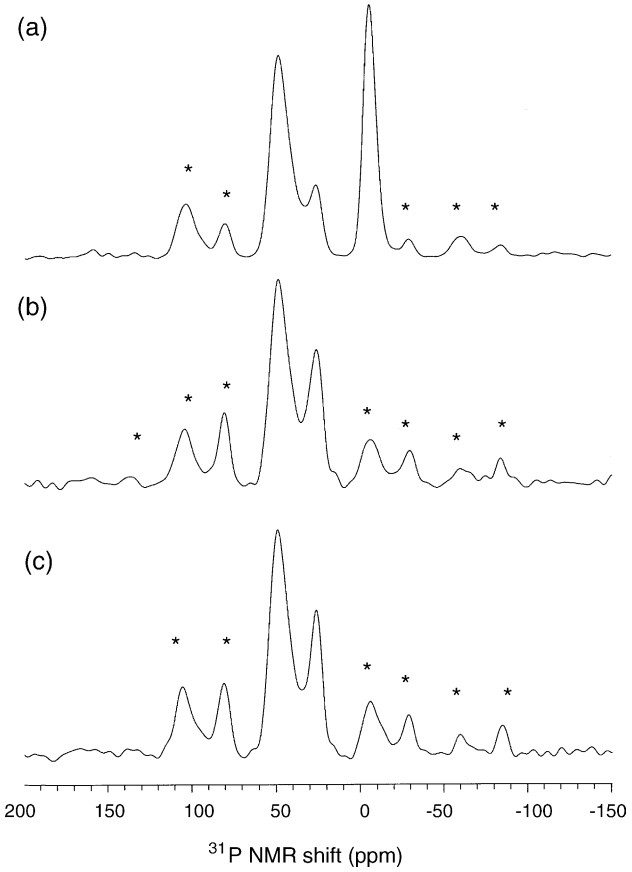

Fig. 7. ^{31}P CPMAS NMR spectra of Fibrecat™ prepared using acetone for the deposition of the Rh precursor: (a) 6-Fibrecat™, 3.1 wt.% P; (b) 4-Fibrecat™, 1.2 wt.% P; and (c) 3-Fibrecat™, 1.2 wt.% P. The spinning sidebands are denoted with asterisks (*).

alone. When the Fibrecat™ was prepared from acetone, the ratio of the monophosphine species to diphosphine species (mono/di) was clearly higher (see Table 1). The highest ratio of 5.6 was obtained with 6-Fibrecat™ (Acet) which contained 3.1 wt.% P. For some reason, not all the styryldiphenylphosphine reacted with the rhodium precursor (Fig. 7a). Using the wt.% P provided by the manufacturer, together with the ratios of the mono, di and unreacted styryldiphenylphosphine peaks in the ^{31}P CPMAS NMR spectra, the amount of Rh expected would be 6.5 wt.%. The method B gave 5.9 wt.% Rh.

The fibre support before and after Rh precursor addition was characterised by DRIFT. The DRIFT spectrum of the polymer matrix before Rh precursor addition shows only a small peak at 1943 cm^{-1} between 1900 and 2030 cm^{-1} (not shown). The spectrum of 4-Fibrecat™ (Fig. 8) shows a peak in the carbonyl region at 1978 cm^{-1}, which is typical for the carbonyl group of Rh(CO)(acac)(PS-PPh$_2$) [32,33]. For 6-Fibrecat™ (Acet) the carbonyl peak is located at 1981 cm^{-1}.

In all, two types of Rh-P species were formed during the preparation of the catalyst. The Rh(acac)(CO)$_2$ precursor was coordinated to the phosphine groups of the support forming Rh-monophosphine and Rh-diphosphine species.

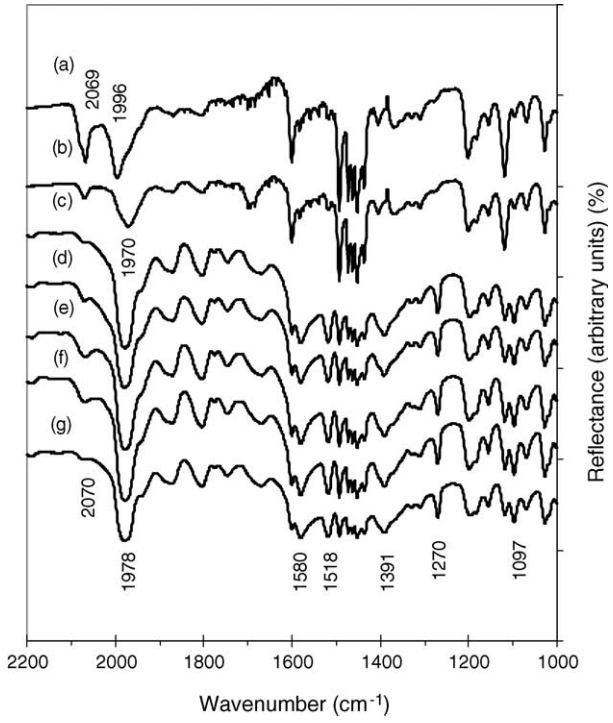

Fig. 8. DRIFT spectra of 4-Fibrecat™ after pretreatment at 110 °C for 7 h with: (a) CO/H$_2$ at 1.0 MPa (diluted sample); (b) CO/H$_2$ at 0.5 MPa (diluted sample); (c) H$_2$ at 1.0 MPa; (d) H$_2$ at 0.5 MPa; (e) CO at 1.0 MPa; (f) CO at 0.5 MPa; (g) fresh 4-Fibrecat™.

The mono/di ratio varied from 1.5 to 5.6 depending on the solvent used in the deposition stage and the phosphorus content of the support. The amount of the monophosphine species was higher when the catalysts were prepared with acetone rather than dichloromethane as solvent. The highest mono/di ratio (5.6) was obtained on the support containing 3.1 wt.% P.

3.2.2. *Characterisations after pretreatments*

The results from the quantitative ^{31}P MAS NMR measurements with 3-Fibrecat™ are presented in Fig. 9. Note that Fig. 9 shows the wt.% of P in each species, not the ratios of the Rh-phosphine species. Fig. 10 shows the fitting of the centre bands of the ^{31}P MAS spectra of the fresh catalyst and the catalyst after treatment with CO/H$_2$. The spinning sidebands were similarly fitted (not shown).

As illustrated in Fig. 11, the ^{31}P CPMAS NMR spectrum of H$_2$-pretreated 4-Fibrecat™ (Fig. 11b) shows no difference relative to the spectrum of the original sample (Fig. 11a). Evidently the pretreatments with CO or CO/H$_2$ convert the Rh(CO)(acac)(PS-PPh$_2$) species to a new species whose peak position is around 35 ppm (Fig. 11c). From the quantitative results (Fig. 9) it can be seen that pretreatment with CO/H$_2$ is more effective than pretreatment with carbon monoxide in converting the acac species to the species at 35 ppm. The diphosphine peak at 28 ppm shifts a little to 26.5 ppm and becomes narrower, perhaps due to some sort of annealing of the polymer matrix. The origin of the shoulder at 35 ppm is discussed below. The ^{13}C CPMAS

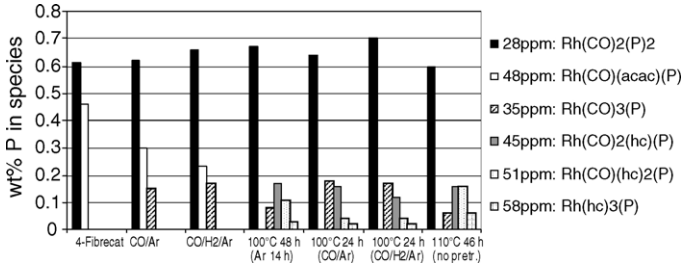

Fig. 9. Distribution of phosphorus-containing species for 3-Fibrecat™ after different pretreatments and after reaction, calculated from ^{31}P MAS NMR measurements (hc: hydrocarbon).

NMR spectrum of 4-Fibrecat™ also confirms that peaks due to acac ligands, at 188 ppm for the carbonyl carbon and 100 ppm for the CH carbon, disappear during CO/H_2 pretreatment (see Fig. 12a and b).

The DRIFT spectra of 4-Fibrecat™ also support the disappearance of acac during CO/H_2 treatment. As illustrated in Fig. 8, the peaks for acac ligand in Rh(acac)CO(PS-PPh_2) at 1580, 1518, 1391, 1270 and 1097 cm^{-1} [32,35,36] disappear almost completely upon CO/H_2 treatment. In accord with the ^{31}P CPMAS NMR spectrum, there was no change in the DRIFT spectrum after H_2 treatment. In contrast to the NMR results, no changes after carbon monoxide treatment were detected by DRIFT spectroscopy.

The carbonyl stretching region of the DRIFT spectra changed after CO/H_2 pretreatment (Fig. 8): the peak at 1978 cm^{-1} disappeared and new peaks appeared at 1970 cm^{-1} (0.5 MPa) or at 1996 cm^{-1} with a shoulder at 1970 cm^{-1} (1.0 MPa). The carbonyl peak at 2069 cm^{-1} was clearly bigger when the pretreatment was carried out at 1.0 MPa and it also had a shoulder at 2078 cm^{-1}. Thus, four

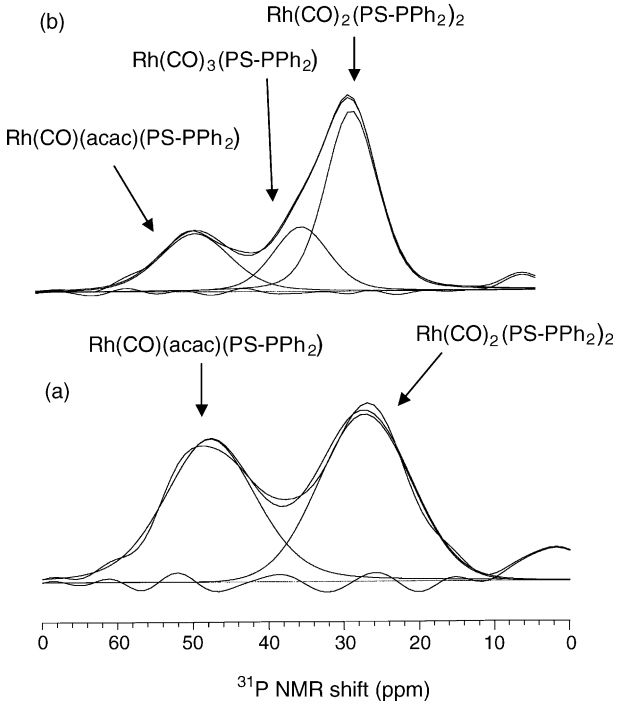

Fig. 10. Fitting of the centre band of the ^{31}P MAS NMR spectra of: (a) 3-Fibrecat™ and (b) 3-Fibrecat™ after CO/H_2 treatment at 100 °C and 0.5 MPa for 7 h.

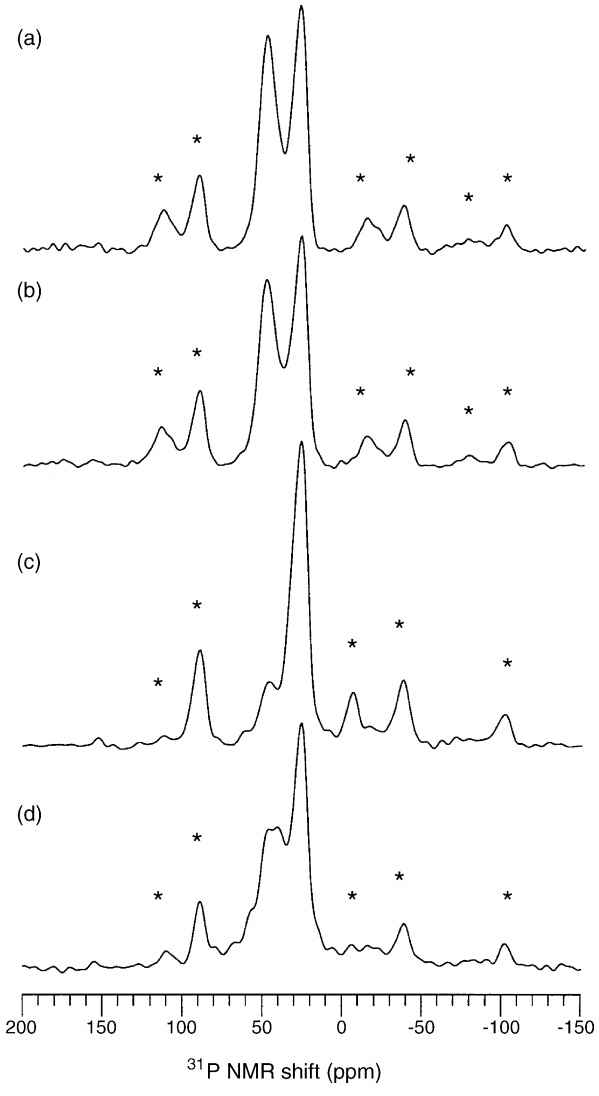

Fig. 11. ^{31}P CPMAS NMR spectra of: (a) 4-Fibrecat™; (b) 4-Fibrecat™ after H_2 pretreatment at 110 °C and 0.5 MPa for 7 h; (c) 4-Fibrecat™ after CO/H_2 pretreatment at 110 °C and 0.5 MPa for 7 h; and (d) 4-Fibrecat™ after reaction at 110 °C and 0.5 MPa for 46 h (Ar:CO:H_2:C_2H_4 = 4:1:1:1, no pretreatment). The spinning sidebands are denoted with asterisks (*).

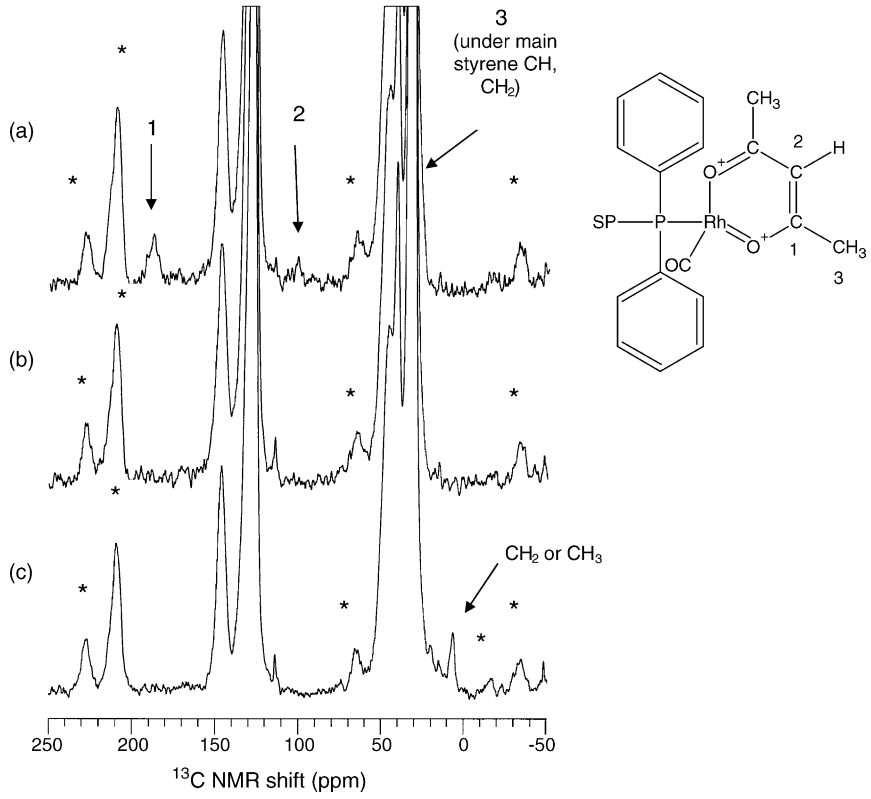

Fig. 12. ^{13}C CPMAS NMR spectra of: (a) 4-Fibrecat™; (b) 4-Fibrecat™ after CO/H_2 pretreatment at 110 °C and 0.5 MPa for 7 h; and (c) 4-Fibrecat™ after reaction at 110 °C and 0.5 MPa for 46 h (Ar:CO:H_2:C_2H_4 = 4:1:1:1, no pretreatment). The spinning sidebands are denoted with asterisks (*).

carbonyl vibrations could be detected at 1.0 MPa. These DRIFT results indicate the formation of a carbonyl species after CO/H_2 treatment.

The disappearance of acac means that either the Rh-acac or P-Rh bond breaks. If the acac-Rh bond breaks, a carbonyl species is formed and Hacac is released. If the P-Rh bond breaks, a $Rh(CO)_2$(acac) species is detached from the support and free phosphine PS-PPh_2 is formed. However, no free styryldiphenylphosphine was observed in the ^{31}P NMR spectra after reaction or pretreatments, which indicates that no phosphorus–rhodium bonds were broken. Quantitative ^{31}P MAS NMR also showed no loss of phosphorus or phosphorus-coordinated rhodium during either reaction or pretreatment, indicating that no Rh was lost in the form of a $Rh(CO)_2$(acac) species. The DRIFT measurements, together with the ^{31}P NMR and ^{13}C NMR measurements suggest that the species at 35 ppm in the ^{31}P NMR spectrum formed during CO and CO/H_2 treatments is $Rh(CO)_3$(PS-PPh_2). It must be noted, however, that the DRIFT and NMR measurements were carried out in air and the actual species present in CO/H_2 atmosphere is probably a carbonyl hydride species, $HRh(CO)_3$(PS-PPh_2).

3.2.3. Characterisations after reaction

In the ^{31}P MAS NMR spectrum of Fibrecat™ after reaction (Fig. 11d), the signal for the diphosphine species is intact at 26.3 ppm, while the signal for Rh(CO)(acac)(PS-PPh_2) at 48.7 ppm changes into a series of overlapping peaks around 40–60 ppm. The ^{13}C CPMAS NMR spectra after reaction (Fig. 12c) shows no peaks for acac but a new peak appears at 7 ppm. This peak could be either CH_2 or CH_3 group and on this basis we propose that a hydrocarbon is coordinated to rhodium. The peaks appearing during reaction at 45–58 ppm might thus be $Rh(PS\text{-}PPh_2)(CO)_{3-z}(C_xH_y)_z$ (z = 1–3) species, where the species with more coordinated hydrocarbons appears at higher frequency. Fig. 13 shows a simulation of the centrebands of the

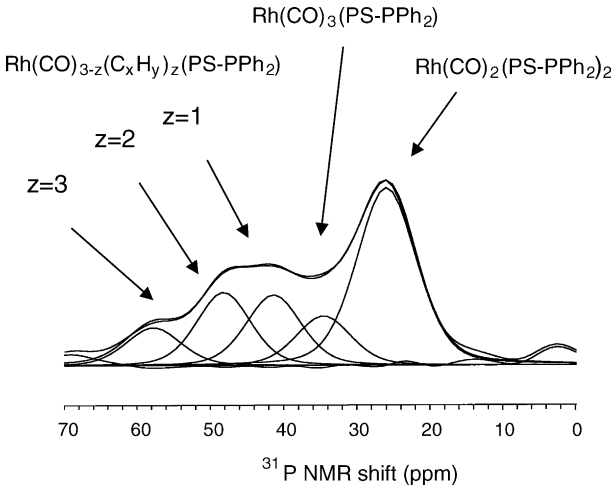

Fig. 13. Fitting of the centre bands of the ^{31}P MAS NMR spectrum of 3-Fibrecat™ after reaction at 110 °C and 0.5 MPa for 46 h (no pretreatment).

3-Fibrecat™ catalyst after reaction. Four peaks were fitted in the 34–58 ppm region in an attempt to separate out the different $Rh(PS\text{-}PPh_2)(CO)_{3-z}(C_xH_y)_z$ ($z = 0$–3) species. The results of using these peak fittings to obtain the amounts of phosphorus in each group are shown in Fig. 9. Due to the severely overlapping nature of the peaks, Fig. 8 should only be taken as a guide to the general behaviour of the species in the catalyst.

After the reaction, the amount of species at 35 ppm is higher with the CO and CO/H_2 treated catalysts than with the catalysts not subjected to pretreatment (see Fig. 9). There are fewer species at 45–58 ppm after the hydroformylation reaction with the CO and CO/H_2 treated catalysts than with the Ar treated or non-pretreated catalysts. The treatment with CO/H_2 thus helps the formation of an active species at 35 ppm, so the initial distribution of the $Rh(PS\text{-}PPh_2)(CO)_{3-z}(C_xH_y)_z$ species is with $z = 0$. During reaction the other $z = 1$–3 species are formed, but the distribution is more to the $z = 0$ side. Without any pretreatment, all the species $z = 0$–3 are gradually formed during the reaction and a more even distribution of the $Rh(PS\text{-}PPh_2)(CO)_{3-z}(C_xH_y)_z$ species results. This means that, for the same reaction time, more of the species at 45–58 ppm are formed for the samples with no pretreatment.

The DRIFT spectra of Fibrecat™ after reaction shows vibrations for 3–4 carbonyl groups independent of reaction pressure, temperature or time on stream (see Fig. 14). The vibrations for the acetyl acetonate ligand have disappeared in the same way as after CO/H_2 pretreatments. The DRIFT results affirm the formation of carbonyl-containing species after reaction, which is in accord with the hypothesis suggested by ^{31}P NMR of the formation of $Rh(PS\text{-}PPh_2)(CO)_{3-z}(C_xH_y)_z$ ($z = 0$–3) species.

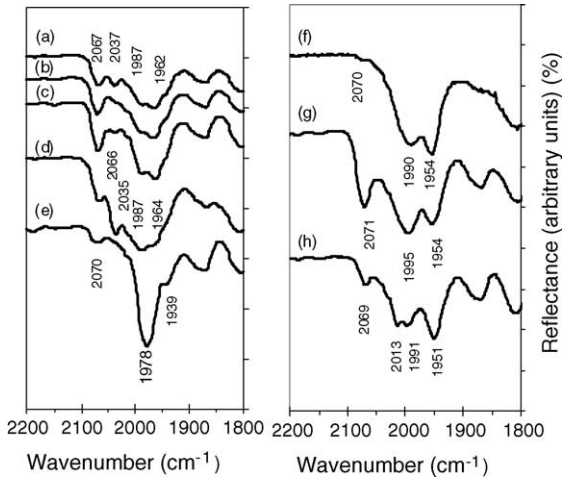

Fig. 14. Carbonyl stretching region of the DRIFT spectra of 3-Fibrecat™ after reaction at 100 °C and 0.5 MPa. The pretreatments before reaction were: (a) Ar; (b) H_2:Ar; (c) CO:Ar; and (d) H_2:CO:Ar for 7 h at 100 °C and 0.5 MPa. (e) DRIFT of fresh 3-Fibrecat™. DRIFT spectra of (f) 8-Fibrecat™ after reaction at 1.0 MPa and 110 °C, feed 14 l/h (4:1:1:1); (g) 4-Fibrecat™ after reaction at 1.0 MPa and 110 °C, feed 13 l/h (10:1:1:1); (h) 4-Fibrecat™ after reaction at 135 °C and 5 bar, feed 3.5 l/h (1:2:2:2).

The quantitative ^{31}P MAS NMR results show that no phosphorus is lost during pretreatment or reaction. The P content for 3-Fibrecat™ measured by quantitative ^{31}P MAS NMR was 1.1 wt.% before and after the reaction. The amount of phosphorus-coordinated rhodium was 2.5 wt.% for the fresh catalyst and 2.4–2.5 wt.% for the catalyst after reaction. Thus, no loss of phosphorus-coordinated rhodium is evident either.

The crystallinity of some of the samples was also estimated from the peak area in the ^{13}C CPMAS NMR spectra at around 33 ppm. This peak area consists of peaks of carbons in the polyethene in the amorphous and crystalline regions of the polymer, and gives some indication of the degree of crystallinity of the polyethene. While the cross-polarisation spectra do not give absolutely quantitative data, we assume that the spectra of different samples can be compared to reveal the relative changes in the peak areas. The crystallinity of the polyethene part of the fibres for 3-Fibrecat™ and 3-Fibrecat™ after CO/H_2 treatment at 100 °C was the same (60%), but after reaction at 110 °C it was slightly higher (65%).

4. Discussion

4.1. Catalyst activation

We propose that two types of Rh-P species were formed during the preparation of Fibrecat™: coordination of the $Rh(acac)(CO)_2$ precursor to the phosphine groups of the support gave rise to a monophosphine species, $Rh(CO)(acac)(PS\text{-}PPh_2)$, and a diphosphine species, $Rh(CO)_2(PS\text{-}PPh_2)_2$. In the Rh/PPh_3-catalysed homogeneous hydroformylation, according to the widely accepted Wilkinson's dissociative mechanism [1,37,38], the active species are 16-electron hydrides, $HRh(CO)(PPh_3)_2$ and $HRh(CO)_2(PPh_3)$, formed by the dissociation of CO from the 18-electron carbonyl hydrides (see Scheme 2).

It was postulated from the characterisation results that, in contact with carbon monoxide, the monophosphine species, $Rh(CO)(acac)(PS\text{-}PPh_2)$, was transformed to a Rh-carbonyl species, $Rh(CO)_3(PS\text{-}PPh_2)$ that is a direct catalyst precursor in hydroformylation. In a similar way, the $Rh(CO)(PPh_3)(acac)/SiO_2$ catalyst needs to lose the acac group before the catalyst becomes active. The activation of the diphosphine species is simpler: all that is required is formation of the carbonyl hydride species, $HRh(CO)_2(PS\text{-}PPh_2)_2$. Accordingly, activation during time on stream occurred only for the phosphine containing catalysts, Fibrecat™ and $2\text{-}Rh\text{-}PPh_3/SiO_2$, while the activity of the supported non-phosphine modified Rh catalysts decreased. The activation period on Fibrecat™ could be shortened by CO or CO/H_2 pretreatments since the catalytic precursor sites were formed during the pretreatment.

Why the conversion level decreased during the CO and CO/H_2 pretreatments remains unclear. If it was due to

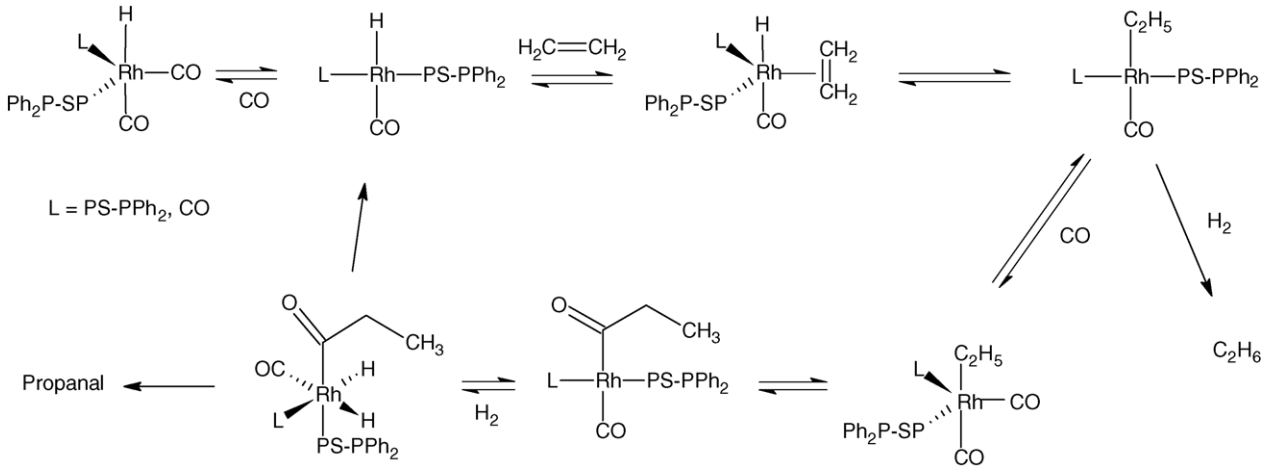

Scheme 2. Wilkinson's dissociative mechanism for rhodium-catalysed ethene hydroformylation.

temperature effects alone, the conversion level should have decreased after Ar pretreatment as well. Since the quantitative ^{31}P NMR shows no loss of phosphorus-coordinated rhodium, the loss in activity cannot be due to loss of rhodium by the formation of volatile carbonyls either.

The excellent activity and selectivity of the fibre-supported rhodium catalysts compared with the other Rh catalysts deserves more detailed discussion. First of all, even though Rh/C and Rh/SiO_2 were highly dispersed and possessed partly reduced rhodium sites favourable for CO insertion [39–41], the activity and selectivity of these catalysts were clearly lower than for Fibrecat™. The characterisations indicate that rhodium was coordinated to the phosphine groups of the fibre, and the resulting sites were active and selective in hydroformylation. Evidently, the active sites are different on fibre and on silica and carbon: isolated Rh-phosphine species are present on fibre and Rh metal clusters on silica and carbon. Furthermore, when the Rh-phosphine species were supported on silica (2-Rh-PPh_3/SiO_2), similar oxo-selectivity was obtained as with rhodium on fibre, but the conversion was only 2%. The rhodium species probably forms large clusters after the solvent removal. The low dispersion of 2-Rh-PPh_3/SiO_2 compared with the isolated active sites on fibre is probably the main reason for the low activity of this catalyst. The active sites at the side chains of the fibre are also more accessible than the active sites in the pores of the silica or active carbon.

Lower reaction pressures and temperatures can be used in homogeneous Rh-phosphine processes, because phosphine groups stabilise the rhodium carbonyl formed [3]. Thus, high activity, similar to our results, is obtained under milder reaction conditions. The high selectivity towards propanal formation compared to hydrogenation is related to the electronic properties of the phosphine ligands. It is well known that the phosphines are strong electron donors; they increase the electron density of the decisive rhodium–carbon bond and, hence, accelerate the migratory insertion of the Rh-alkyl to the carbonyl [42], which improves the hydroformylation selectivity versus hydrogenation.

4.2. Catalyst deactivation

The two main deactivation mechanisms in homogeneous hydroformylation are the degradation of the phosphine ligands and the oxidation of the phosphine ligands to phosphine oxide [43]. Degradation of the phosphine ligands is not probable under the mild reaction conditions we used. Also, the quantitative ^{31}P NMR did not show loss of phosphorus even after 50 h reaction. The formation of Rh-dimers observed in homogeneous processes can be prevented by immobilisation of the catalyst on a support [43] and is therefore not probable on Fibrecat™.

Feldman and Orchin [21] noticed that the presence of oxygen resulted in the formation of triphenylphosphine oxide and loss of catalytic activity on a membrane-supported Rh-phosphine catalyst. There might have been traces of oxygen present in the system when the reaction was started, so one should consider the possibility of oxidation of phosphine resulting in breakage of the Rh-P bond. However, examination of the ^{31}P NMR spectra shows that the ratio of the two different relaxation time components for the peak at 28 ppm, before and after CO/H_2 treatment does not change significantly. We have assumed that the minority, faster relaxing component comes from phosphine oxide in the catalyst. If this is valid then it is reasonable to assume that there is no phosphine oxide formed during the reaction either. Moreover, the quantitative ^{31}P NMR results show that there was no loss of coordinated rhodium or phosphorus during the pretreatments or reaction.

After the initial activation period, and after reaching the steady-state level, the activity of Fibrecat™ decreased slightly with time. The ^{31}P NMR spectra of Fibrecat™ after the reaction showed new peaks at around 40–60 ppm and these were assigned to $Rh(CO)_{3-z}(C_xH_y)_z(PS\text{-}PPh_2)$ (z = 1–3) species. These complexes were formed after both 24 and 50 h on stream, but the amount of the species with higher z increased with time. The amount of hydrocarbon coordination was also higher at 110 °C than at 100 °C (see Fig. 9). As a result of coordination of two or three

hydrocarbons, there are not enough coordination sites for carbonyl, hydrogen and ethene (step 2 in Scheme 1) and the amount of active sites available for hydroformylation decreases. The increased coordination of hydrocarbon with time at least partly explains the decrease in activity.

One option for the coordinated species would be the ethyl group, since ethyl coordination to rhodium is part of the catalytic cycle (Scheme 2), even though it is further hydroformylated to propanal or hydrogenated to ethane. Other possible hydrocarbons are reaction products, and parts of the acetyl acetonate group, which might have decomposed in contact with CO/H_2 [44].

The deactivation was clearer at 110 °C than at 100 °C. Samples were exposed to temperatures just around the melting point of polyethene for a long time and then cooled fairly slowly and this could have caused annealing of the sample [45]. The possible annealing was studied by examining the CH_2 carbon region around 33 ppm in the ^{13}C NMR spectra to get a qualitative idea of the degree of crystallinity of the polyethene. No annealing was observed in 3-Fibrecat™ after CO/H_2 treatment at 100 °C. After reaction at 110 °C and 0.5 MPa, however, the crystallinity of the catalyst was increased indicating that some annealing of the fibres had occurred during the reaction. Thus, annealing could also be another contribution to the clearer deactivation of Fibrecat™ at 110 °C compared to 100 °C. The increase in crystallinity makes active sites in the amorphous phase less accessible for the reactants, resulting in a decrease in activity. As discussed above, the amount of hydrocarbon coordination with $z = 2$ or 3 was also higher, contributing to the deactivation at 110 °C.

One should also remember that, at the low temperature employed, some of the products, especially C_6O, even though formed in small quantities, may over time accumulate on the support of the catalyst and block part of the active sites.

By way of summary, the catalytic results and characterisations indicate that the deactivation on Fibrecat™ was caused by formation of inactive Rh-species by coordination of hydrocarbon on the active species, annealing of the polyethene support at 110 °C, and possibly by accumulation of reaction products on the surface with time. The amount of phosphorus or coordinated rhodium did not decrease during the reaction.

5. Summary

Polyethene fibre-supported Rh-phosphine catalyst, Fibrecat™, was successfully applied for ethene hydroformylation: high propanal selectivity and high activity were obtained under mild reaction conditions of 100 °C and 0.5 MPa. The supported Rh-phosphine species effectively directed the selectivity towards propanal with 95% selectivity. A considerable amount of hydrogenation took place on the non-phosphine-modified Rh catalysts.

The ^{31}P NMR characterisations suggested the formation of both a monophosphine species, $Rh(acac)(CO)(PS\text{-}PPh_2)$, and a diphosphine species, $Rh(CO)_2(PS\text{-}PPh_2)_2$, on Fibrecat™. The acac detaches from the Rh-monophosphine species during pretreatment of the catalyst with CO, and still more effectively with CO/H_2. The activation period at the beginning of the reaction can be explained by the formation of the active Rh-carbonyl hydrides, $HRh(CO)_3(PS\text{-}PPh_2)$ and $HRh(CO)_2(PS\text{-}PPh_2)_2$.

Fibrecat™ was stable for 24 h at 100 °C and 0.5 MPa, but some deactivation occurred during 50 h. Deactivation was probably caused by the formation of inactive Rh-phosphine species by coordination of hydrocarbon on the active Rh-species. The accumulation of reaction products on the fibre support with time can also not be ignored. At higher temperature (110 °C), deactivation was probably caused also by annealing of the polyethene fibres. No phosphorus or phosphorus-coordinated rhodium was lost during pretreatment or reaction.

Acknowledgements

Funding was received from the Academy of Finland through the Graduate School in Chemical Engineering and from the Nordic Council of Ministers through the Nordic Energy Research Program.

References

[1] C.D. Frohning, C.W. Kohlpaintner, in: B. Cornils, W.A. Herrmann (Eds.), Applied Homogeneous Catalysts with Organometallic Compounds, vol. 1, VCH, Weinheim, 1996 (Chapter 2.1).
[2] P.W.N.M. Van Leeuwen, C. Claver (Eds.), Rhodium Catalyzed Hydroformylation, in Catalysis by Metal Complexes, Kluwer Academic Publishers, Dordrecht, Netherlands, 2000, p. 284.
[3] V.A. Likholobov, B.L. Moroz, in: G. Ertl, H. Knözinger, J. Weitkamp (Eds.), Handbook of Heterogeneous Catalysis, vol. 5, VCH, Weinheim, 1997 (Chapter 4.5).
[4] T.A. Kainulainen, M.K. Niemelä, A.O.I. Krause, J. Mol. Catal. A: Chem. 122 (1997) 39.
[5] W. Junfan, S. Juntan, L. Hong, H. Binglin, React. Polym. 12 (1990) 177.
[6] M. Lenarda, L. Storaro, R. Ganzerla, J. Mol. Catal. A: Chem. 111 (1996) 203.
[7] L. Huang, Y. Xu, W. Guo, A. Liu, D. Li, X. Guo, Catal. Lett. 32 (1995) 61.
[8] W.M.W. Sachtler, M. Ichikawa, J. Phys. Chem. 90 (1986) 4752.
[9] T.A. Kainulainen, M.K. Niemelä, A.O.I. Krause, J. Mol. Catal. A: Chem. 140 (1999) 173.
[10] T.A. Kainulainen, M.K. Niemelä, A.O.I. Krause, Catal. Lett. 53 (1998) 97.
[11] P. Terreros, E. Pastor, J.L.G. Fierro, J. Mol. Catal. 53 (1989) 359.
[12] C.U. Pittman Jr., R.M. Hanes, J. Am. Chem. Soc. (1976) 5402.
[13] K.G. Allum, R.D. Hancock, I.V. Howell, R.C. Pitkethly, P.J. Robinson, J. Organomet. Chem. 87 (1975) 189.
[14] C.U. Pittman Jr., L.R. Smith, R.M. Hanes, J. Am. Chem. Soc. (1975) 1742.
[15] C.U. Pittman Jr., W.D. Honnick, J. Org. Chem. 45 (1980) 2132.

[16] T. Jongsma, P. Kimkes, G. Challa, P.W.N.M. van Leeuwen, Polymer 33 (1992) 161.
[17] E. Bonaplata, H. Ding, B.E. Hanson, J.E. McGrath, Polymer 36 (1995) 3035.
[18] K.S. Ro, S.I. Woo, J. Mol. Catal. 61 (1990) 27.
[19] G.O. Evans, C.U. Pittman Jr., R. McMillan, R.T. Beach, R. Jones, J. Organomet. Chem. 67 (1974) 295.
[20] F.R. Hartley, S.G. Murray, P.N. Nicholson, J. Mol. Catal. 16 (1982) 363.
[21] J. Feldman, M. Orchin, J. Mol. Catal. 63 (1990) 213.
[22] Y. Zhang, H.-B. Zhang, G.-D. Lin, P. Chen, Y.-Z. Yuan, K.R. Tsai, Appl. Catal. A: Gen. 187 (1999) 213.
[23] J.H. Näsman, M.J. Sundell, K.B. Ekman, US Patent 5326825 (5 July 1994).
[24] Johnson Matthey plc, Orchard Road, Royston, Hertfordshire, SG85HE, United Kingdom.
[25] A. Guyot, P. Hodge, D.C. Sherrington, H. Widdecke, React. Polym. 16 (1991–1992) 233.
[26] R.S. Karinen, A.O.I. Krause, K. Ekman, M. Sundell, R. Peltonen, Stud. Surf. Sci. Catal. 130 (2000) 3411.
[27] J. Lilja, J. Aumo, T. Salmi, D.Y. Murzin, P. Mäki-Arvela, M. Sundell, K. Ekman, R. Peltonen, H. Vainio, Appl. Catal. A: Gen. 228 (2002) 253.
[28] P. Mäki-Arvela, T. Salmi, M. Sundell, K. Ekman, R. Peltonen, J. Lehtonen, Appl. Catal. A: Gen. 184 (1999) 25.
[29] Smoptech Ltd., Virusmäentie 65 A, FIN-20300 Turku, Finland.
[30] M.E. Halttunen, M.K. Niemelä, A.O.I. Krause, T. Vaara, A.I. Vuori, Appl. Catal. A: Gen. 205 (2001) 37.
[31] P.E. Shestakova, T.G. Cherkasova, I.S. Podkorytov, Yu.S. Varshavsky, Rhodium Express 7–8 (1994) 17.
[32] F. Bonati, G. Wilkinson, J. Chem. Soc. (1964) 3156.
[33] P.E. Garrou, G.E. Hartwell, Inorg. Chem. 15 (1976) 646.
[34] T. Malmström, C. Andersson, J. Hjortkjaer, J. Mol. Catal. A: Chem. 139 (1999) 139.
[35] I.V. Babich, Y.V. Plyuto, P. Van Der Voort, E.F. Vansant, J. Colloid Interf. Sci. 189 (1997) 144.
[36] M. Mikami, I. Nakagawa, T. Shimanouchi, Spectrochim. Acta 23A (19671037).
[37] B. Breit, W. Seiche, Synthesis (1) (2001) 1.
[38] J. Falbe (Ed.), New Syntheses With Carbon Monoxide, Springer-Verlag, Berlin, Heidelberg, 1980, p. 465.
[39] L. Huang, Y. Xu, W. Guo, A. Liu, D. Li, X. Guo, Catal. Lett. 32 (1995) 61.
[40] W.M.H. Sachtler, M. Ichikawa, J. Phys. Chem. 90 (1986) 4752.
[41] S.S.C. Chuang, S.-I. Pien, J. Catal. 135 (1992) 618.
[42] A. Caiazzo, R. Settambolo, L. Pontorno, R. Lazzaroni, J. Organomet. Chem. 599 (2000) 298.
[43] P.W.N.M. van Leeuwen, Appl. Catal. A: Gen. 212 (2001) 61.
[44] A. Hakuli, A. Kytökivi, Phys. Chem. Chem. Phys. 1 (1999) 1607.
[45] J.M.G. Cowie, Polymers: Chemistry and Physics of Modern Materials, second ed. Blackie Academic & Professional, London, 1991, p. 436.